Available online at www.sciencedirect.com
ScienceDirect
Computers and Geotechnics 34 (2007) 92–103
COMPUTERS AND GEOTECHNICS
www.elsevier.com/locate/compgeo

Particle swarm optimization algorithm for the location of the critical non-circular failure surface in two-dimensional slope stability analysis

Y.M. Cheng [a,*], Liang Li [a,b], Shi-chun Chi [b], W.B. Wei [a]

[a] *Department of Civil and Structural Engineering, Hong Kong Polytechnic University, Hong Kong*
[b] *School of Civil and Hydraulic Engineering, Da Lian University of Technology, China*

Received 9 March 2006; received in revised form 6 October 2006; accepted 18 October 2006
Available online 27 December 2006

Abstract

Locating the critical slip surface with the minimum factor of safety of a slope is a difficult N-P type optimization problem. In recent years, some modern global optimization methods have been developed with success in treating various types of problems, but very few of these methods have been applied to geotechnical problems. In this paper, use of a modified particle swarm optimization method with a termination criterion is proposed. The proposed algorithm is demonstrated to be effective and efficient in solving complicated problems with a high level of confidence.

Keywords: Particle swarm; Global optimization; Factor of safety; Control variables

1. Introduction

Slope stability analysis is a classical problem but is still attracting the attention of many engineers and researchers. At present, the limit equilibrium method is widely used by engineers and researchers, as the factor of safety can be estimated without the knowledge of the initial stress conditions and a problem can be defined and solved within a relatively short time. Besides the limit equilibrium method, the limit analysis method has also been used for simple problems [7], but its application to complicated real problems is still limited, and it is seldom adopted for routine analysis and design.

The use of both the limit equilibrium and the limit analysis methods for general problems requires the selection of trial failure surfaces and the minimization of the factor of safety. For a general non-circular failure surface, the number of control variables is much more than three, and the use of the geometric method by grid is not practical. Some of the difficulties in the location of the general critical non-circular failure surfaces are

1. The objective function of the safety factor f is usually non-smooth, non-convex and may not be continuous over the whole solution domain. Gradient type optimization methods may break down easily if 'failure to converge' (i.e., no solution for f for some combinations of control variables) is encountered, which can occur for complicated ground conditions with external loads.
2. Chen and Shao [8] have found that multiple minima will exist in the general case, and many solution methods can be trapped easily by the existence of a local minimum unless a good initial trial can be chosen for the analysis. The case studies in the present paper will illustrate the importance of the local minimum in the global minimization analysis.
3. A good initial trial failure surface for the global minimization is usually difficult to estimate for general conditions. Without a good initial trial, most of the classical minimization methods will fail to locate the global minimum.

* Corresponding author.
E-mail address: ceymchen@polyu.edu.hk (Y.M. Cheng).

0266-352X/$ - see front matter © 2006 Elsevier Ltd. All rights reserved.
doi:10.1016/j.compgeo.2006.10.012

Due to the development of various activities, many slopes are formed in various cities, and different types of slope stabilization measures have been adopted. The increased complexities of the slope stability analyses have drawn the attention of many researchers and engineers, who seek to find effective and efficient methods for determining the global minimum factor of safety for complex problems. Baker and Garber [2] and Baker [3] used the calculus of variations to locate the critical slip surface and its associated factor of safety, but this approach is too complicated for real engineering problems. Various methods have been used by different researchers: the simplex method by Nguyen [14] and Chen and Shao [8]; alternating variable methods by Celestino and Duncan [6]; the conjugate-gradient method by Arai and Tagyo [1]; the Monte-Carlo method by Greco [10] and Malkawi et al. [13]. These methods are applicable for simple problems but can be trapped by the presence of a local minimum for general cases.

Among the modern heuristic global optimization methods that have evolved in recent years, there have been only limited applications in geotechnical engineering. The simulated annealing method has been adopted by Cheng [9], while the genetic algorithm and the leap-frog algorithm have been adopted by Zolfaghari et al. [20] and Bolton et al. [5], respectively. In past studies using the heuristic global optimization methods, the control variables were defined over static bounds, except for the algorithm by Cheng [9] where the bounds are dynamic and are controlled by the requirement of a kinematically acceptable failure mechanism.

Global optimization problems are typically difficult to solve and, in the context of combinatorial problems, they are often N-P hard problems. Global optimization problems fall within the broader class of nonlinear programming problems. In recent years, some new artificial intelligence based global optimization methods have been developed for signal processing and pattern recognition that are worth considering for application to the slope stability problem where the objective function may be a discontinuous function. In this paper, a procedure based on a modified particle swarm optimization is proposed, and the method of generating failure surfaces is similar to that by Greco [10], Malkawi et al. [13] and Cheng [9]. The numerical studies in the examples have demonstrated that the proposed method is efficient and effective for many complicated and difficult problems.

2. Generation of a trial slip surface

To locate the critical non-circular failure surface, a trial slip surface generation algorithm is required. Take the Cartesian system of reference Oxy as shown in Fig. 1 for reference. The ground profile is represented by the function $y = y_1(x)$, and the water table is represented by the function $y = w(x)$. The bed rock surface is represented by the function $y = R(x)$, while functions, $y = l_i(x)$ can be introduced

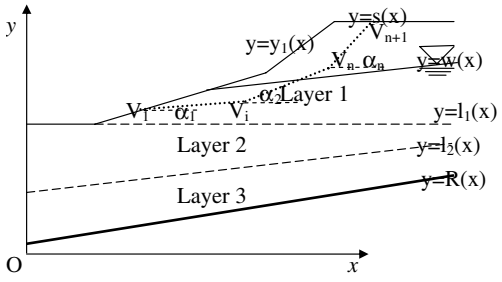

Fig. 1. Defining a slip surface.

to represent the boundaries between different soil layers. The slip surface is described using the function $y = s(x)$.

The method of slices requires the failure soil mass to be divided into n vertical slices, and the slip surface is represented by $n + 1$ vertices $[V_1, V_2, \ldots, V_{n+1}$ with coordinates (x_1, y_1), (x_2, y_2), …, (x_{n+1}, y_{n+1}), respectively]. Each slice can be identified by two adjacent vertices. In general, the potential slip surfaces are concave upward (kinematically acceptable requirement) with only few exceptions. The concave upward requirement can be formulated as follows:

$$\alpha_1 \leqslant \alpha_2 \leqslant \cdots \leqslant \alpha_n \tag{1}$$

where α_i means the inclination of the base of slice i. Every slip surface can be identified by the control variable vector $\mathbf{X}$

$$\mathbf{X} = [x_1, y_1, x_2, y_2, \ldots, x_n, y_n, x_{n+1}, y_{n+1}]^{\mathrm{T}} \tag{2}$$

The variables y_1 and y_{n+1} can be determined from the slope geometry and the variables x_1 and x_{n+1}, hence y_1 and y_{n+1} are not independent control variables. There are altogether $2n$ independent control variables for the description of a slip surface with $n + 1$ vertices and n slices.

For simplicity, for the failure surface as shown in Fig. 2, the horizontal distance between x_1 and x_{n+1} can be subdivided into n equal segments using

$$x_i = x_1 + \frac{x_{n+1} - x_1}{n} \times (i - 1), \quad i = 2, \ldots, n \tag{3}$$

Alternatively, some of the x-ordinates can be controlled by the turning points of the ground profile while additional x-ordinates are inserted by even division. The remaining control variables are now only $x_1, y_2, \ldots, y_n, x_{n+1}$, where

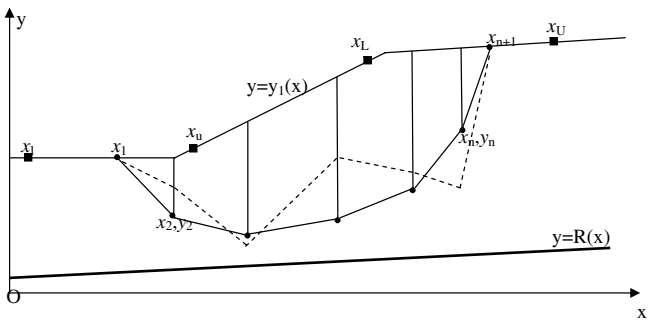

Fig. 2. The control variables for a slip surface.

$R(x_i) < y_i < y_1(x)$, $i = 2, \ldots, n$. The solution domains for the two variables x_1 and x_{n+1} can be defined easily by engineering experience, or sufficiently wide domains can be specified by the engineers. As illustrated in Fig. 2, the value of x_1 varies from x_l to x_u, and x_{n+1} from x_L to x_U. During the search for the critical slip surface, the trial slip surfaces are usually generated randomly and an inadmissible slip surface, as shown in Fig. 2, may be generated. Rectifying procedures are necessary to render the trial slip surface kinematically acceptable, and the procedures in this paper are similar to those proposed by Greco [10] and Malkawi et al. [13]. Consider the slip surface of four slices and five vertices shown in Fig. 3; eight control variables are required: x_1, x_5, β_1, β_5, δ_5, δ_6, δ_7 and δ_8. The vector $\mathbf{V} = (x_1, x_5, \beta_1, \beta_5, \delta_5, \ldots, \delta_8)$ represents a slip surface, where $\beta_1 = \alpha_1 + \frac{\pi}{2}$, $\beta_5 = \alpha_5 + \frac{\pi}{2}$. $\delta_5, \ldots, \delta_8$ are random numbers in the range $(-0.5, 0.5)$. The trial slip surface as shown in Fig. 3 with solid lines is identified by using the vector $\mathbf{V} = [x_1, x_5, \beta_1, \beta_5, 0.0, 0.0, 0.0, 0.0]^T$.

Once the values of the first four variables in $\mathbf{V}$ are given, the two vertices V_1, V_5 and the temporary vertex V'_6 can be obtained as shown in Fig. 3. The midpoints of the line between V_1 and V'_6 and the line between V_5 and V'_6 can then be located. δ_5 is the ratio of the difference between the x-ordinates of V_2 and the midpoint to the difference between the x-ordinates of V_1 and V'_6. Similarly, for δ_6, the three adjacent vertices of the largest horizontal distance can be determined (for example V_2, V'_7 and V_5 in Fig. 3). By using δ_7 and δ_8, we can locate V_3 and V_4 as for V_2, and V'_7. The procedure continues until the specified number of vertices or slices is reached. The lower bounds and the upper bounds to β_1 and β_5 are named $\beta_{1\min}$, $\beta_{1\max}$ and $\beta_{5\min}$, $\beta_{5\max}$, respectively. In summary, the trial slip surfaces of n slices and $n+1$ vertices can easily be obtained by using the step–by-step generation and the vector $\mathbf{V} = (x_1, x_{n+1}, \beta_1, \beta_{n+1}, \delta_5, \ldots, \delta_{2n})$, and the generated failure surfaces will always be kinematically admissible. The above procedures are applicable in most cases as the critical slip surface is usually convex for normal problems. However, there are cases where the critical failure surfaces are non-convex, and the above procedures will need minor modification so that non-convex surfaces can be generated if required. This can be achieved easily by just removing the requirement on the lower bound of each control variable.

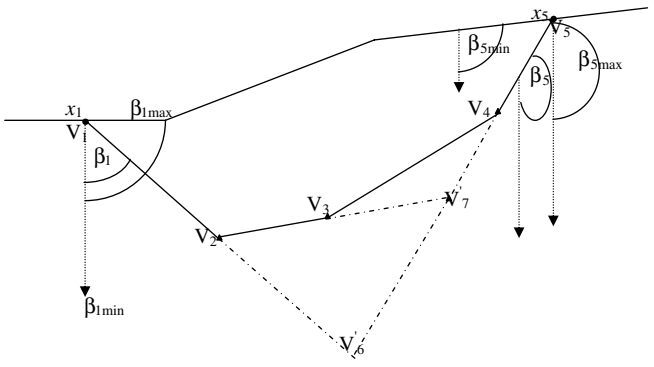

Fig. 3. Proposed procedure for generating an acceptable trial slip surface.

The minimization of the factor of safety and the location of the critical slip surface can now be formulated as follows:

$$\begin{aligned} \min \quad & f(\mathbf{X} \leftarrow \mathbf{V}) \\ \text{s.t.} \quad & x_l \leqslant x_1 \leqslant x_u, \quad x_L \leqslant x_{n+1} \leqslant x_U \\ & \beta_{1\min} < \beta_1 < \beta_{1\max}, \quad \beta_{n+1\min} < \beta_{n+1} < \beta_{n+1\max} \\ & -0.5 < \delta_i < 0.5, \quad i = 5, \ldots, 2n \end{aligned} \tag{4}$$

3. Particle swarm optimization

Particle swarm optimization (PSO) is a heuristic global optimization algorithm developed by Kennedy and Eberhart [12]. This method has been broadly applied in continuous and discrete optimization problems. The PSO method is recognized as an effective method for global optimization and has received great attention in systems and control engineering, automatic recognition, radio systems, etc. Yin [19] proposed a hybrid version of the PSO for the optimal polygonal approximation of digital curves; Salman et al. [16] adopted PSO for the task assignment problem; Ourique et al. [15] used PSO for dynamic analysis in chemical processes. This method does not require much computer memory while the speed of computation is relatively fast. There are extensive applications of the PSO method in various disciplines, but this method has never been used in geotechnical engineering up to the present.

PSO is based on the simulation of simplified social models, such as bird flocking, fish schooling, and the swarming theory. It is related to evolutionary computation procedures and has strong ties with the genetic algorithms. This method is developed on a very simple theoretical framework and can be implemented easily with only primitive mathematical operators. In PSO, a group of particles (generally double the number of the control variables, M), referred to as the candidates or potential solutions [given as $\mathbf{V}$ in Eq. (5)], are flown in the problem and search the space to determine their optimum position. This optimum position is usually characterized by the optimum value of a fitness function (e.g., factor of safety for the present problem). Each "particle" is represented by one vector in the multidimensional space to characterize its position ($\mathbf{V}_i^k$), and another vector to characterize its velocity ($\mathbf{W}_i^k$) at the current time step k. The algorithm assumes that particle i is able to carry out simple space and time computations in order to respond to the quality of the environmental factors. That is, a group of birds can determine the average direction and the speed of flight during the search for food, based on the amount of food normally found in certain regions of the space. The results obtained at the current time step k can be used to update the positions of the next time step. It is also assumed that the group of particles is

able to respond to the environmental changes. In other words, after finding a good source of food in a certain region of the space, the group of particles will take this new piece of information into the consideration to formulate the 'flight plan'. Therefore, the best results obtained throughout the current time step are considered to generate the new set of positions for the whole group.

In order to pursue the optimum of the fitness function, the velocity $\mathbf{W}_i^k$, and hence the position $\mathbf{V}_i^k$, of each particle is adjusted in each time step. The updated velocity $\mathbf{W}_i^{k+1}$ is a function of three major components:

1. the old velocity of the same particle ($\mathbf{W}_i^k$);
2. the difference between the ith particle's best position found so far (called $\mathbf{P}_i$) and the current position;
3. the difference between the best position of any particle within the context of the topological neighborhood of the ith particle found so far (called P_g—its objective function value is f_g) and the current position of the ith particle $\mathbf{V}_i^k$.

Each of the components 2 and 3 mentioned above is stochastically weighted and added to component 1 to update the velocity of each particle with enough oscillations to empower each particle to search for a better pattern within the problem space. In brief, each particle employs Eq. (5) to update its position

$$\begin{aligned}\mathbf{W}_i^{k+1} &= \omega\mathbf{W}_i^k + c_1 r_1(\mathbf{P}_i - \mathbf{V}_i^k) + c_2 r_2(\mathbf{P}_g - \mathbf{V}_i^k)\\ \mathbf{V}_i^{k+1} &= \mathbf{V}_i^k + \mathbf{W}_i^{k+1}\\ i &= 1, 2, \ldots, 2n\end{aligned} \tag{5}$$

where c_1 and c_2 are responsible for introducing the stochastic weighting to components 2 and 3, respectively. These parameters are commonly chosen to be 2, which will also be used in this study. r_1 and r_2 are random numbers in the range $[0, 1]$. ω is the inertia weight coefficient. A larger value for ω will enable the algorithm to explore the search space, while a smaller value of ω will lead the algorithm to exploit the refinement of the results. The flow chart for the PSO in searching for the critical slip surface is shown in Fig. 4.

The termination criterion for the PSO is not stated explicitly by Kennedy and Eberhart [12] (the same is true for many other modern global optimization methods). Usually a fixed number of trials is carried out, with the minimum value from the trials taken as the global minimum. Since the number of trials is not known in advance, engineers are required to try different numbers of trials, and the minimum value from the different trials is selected as the global minimum. This is a major limitation of the original PSO (and of many other global optimization methods), which will be improved in this study. In the present proposal, if $\mathbf{P}_g$ remains unchanged after N_{iter} iterations are performed, the algorithm terminates. Namely, if Eq. (6) is satisfied, the search algorithm will terminate

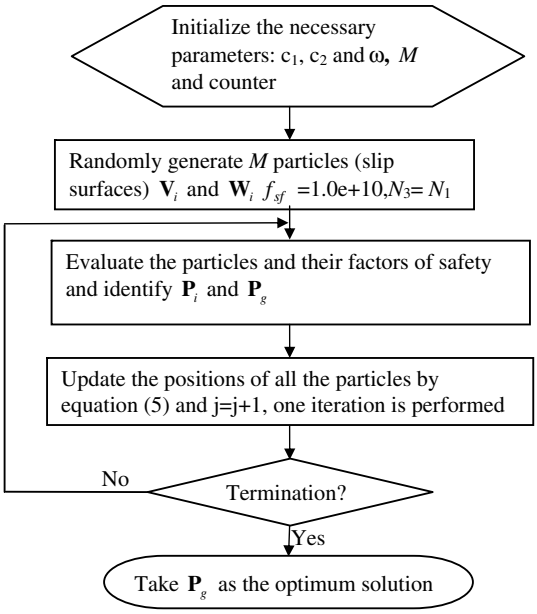

Fig. 4. Flow chart for the particle swarm optimization.

$$\left|f(\mathbf{P}_{g,\text{old}}) - f(\mathbf{P}_g)\right| \leqslant \varepsilon \tag{6}$$

In Eq. (6), $\mathbf{P}_g$ represents the optimum of the group at the current iteration N_1, $\mathbf{P}_{g,\text{old}}$ means the optimum of the group at iterations N_2 ($N_2 = N_1 - N_{\text{iter}}$), and ε is the tolerance for the termination of the analysis, which is chosen as 0.0001 in the present study. The number of objective function evaluations, denoted as NOF, can indicate the time required for the optimization algorithm during the search for the critical slip surface. During the present study, the parameters adopted are $c_1 = c_2 = 2.0$, $\omega = 0.5$, $M = 4n$ and $N_{\text{iter}} = 200$. The adoption of different default parameters is also required for other global optimization methods, and this is a major problem for general global optimization analysis. Based on extensive tests, we have found that the capability of PSO is not sensitive to these default parameters.

4. Modified particle swarm optimization algorithm

If the number of slices (or the number of control variables) is large, the number of trials required by the original PSO will be large. To obtain the optimized solution with fewer evaluations, we propose a new version of PSO called Modified PSO (MPSO). In MPSO, only several flies within the whole group of particles are allowed. In addition, particles with better objective function values are allowed to fly more within one iteration step than those with worse objective function values. The following flying procedures are implemented:

(1) Several flies are now performed instead of one fly for each particle in the group. Herein, suppose N_a ($\leqslant M$) flies are allowed in MPSO within each iteration step. In addition, one particle can fly more than one time according to its objective function value. In this study, the better

the objective function value of one particle, the more times it can fly. A parameter η ($0 < \eta < 1.0$) is used to implement the above procedure of fly. The current M particles are sorted by ascending order in terms of the objective function values, and the probability of each particle flying (namely the flying probability) is determined according to

$$\begin{cases} \mathrm{pr}_i = (1.0-\eta)^{i-1} \times \eta \\ i = 1, 2, \ldots, M \end{cases} \tag{7}$$

where pr_i means the flying probability of the ith particle. The accumulated probability is represented by the array AP(i)

$$\begin{cases} \mathrm{AP}(i) = \sum_{j=1}^{i} \mathrm{pr}(j) \\ i = 1, 2, \ldots, M \end{cases} \tag{8}$$

A random number r_0, falling within the range from 0 to AP(M), is generated. If $\mathrm{AP}(i-1) < r_0 \leqslant \mathrm{AP}(i)$, then the ith particle will fly one time. It must be noted that after the ith particle flies to the new position, it will go back to the current position and the velocity will remain unchanged.

(2) After N_a flies are completed, the following procedure is checked particle by particle. If one particle has the chance to fly more than one time, a new position and a new velocity is randomly chosen for the next iteration and other positions will be assigned to those having no chances to fly in the current iteration. This procedure is called the updating rule of the MPSO.

Fig. 5 is the flow chart for the proposed MPSO algorithm for a given value of N_a. f_{sf}, $\mathbf{V}_{sf}$ are used to restore the objective function value of the optimum solution and the optimum solution found so far. The initial value of the objective function (factor of safety) f_{sf} is set to a large number in this study, say 1.0e+10. The parameters N_1, N_2, N_3 are used to decide the termination criterion. j_1, j_2 are used to calculate the value of η. In the following case studies, the MPSO adopts the same parameters as the original PSO for comparison purposes.

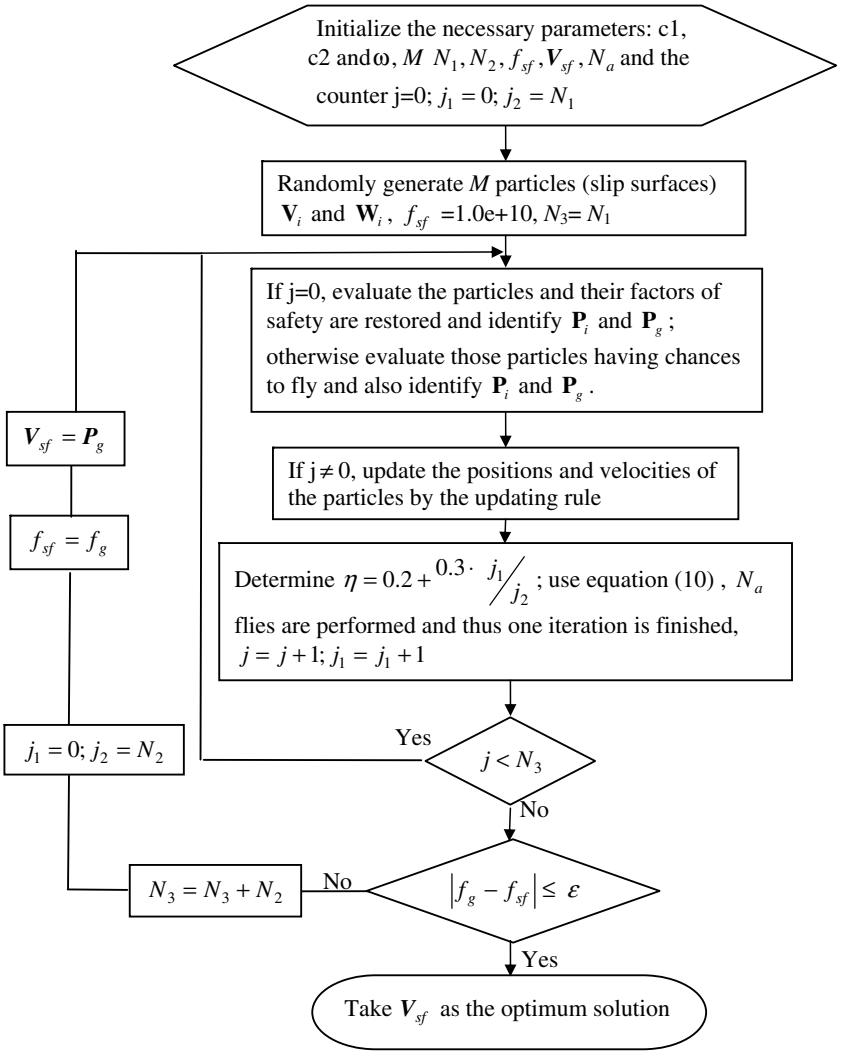

Fig. 5. Flow chart for the modified particle swarm optimization.

5. Numerical examples

Most of the existing global optimization methods can work well for relatively simple problems, as we have found through internal studies (not shown). Cheng [9] has shown there is a solution region cluster around the critical slip surface within which the objective function value is nearly stationary. In this respect, there is not a strong need to determine a very precise location of the critical slip surface. However, when the problem is complicated in geometry with major differences in the soil parameters between different soils, the solution will be sensitive to the precise location of the critical failure surface. The effectiveness and efficiency of the solution algorithm and the capability of the optimization algorithms to escape from the local minima will become important, and these are the foci of the numerical studies in this section. To illustrate the effectiveness of the proposed algorithm, several published examples are considered. It should be pointed out that the success of the optimization algorithm will depend on the correct evaluation of the objective function. Unrealistic factors of safety (objective functions) may appear in the evaluations of the objective function, and the internal forces between the slices should be checked before the factors of safety are accepted.

Example 1 is taken from the work of Malkawi et al. [13]. It is a homogeneous slope and the geotechnical parameters are: friction angle $\phi' = 10°$, cohesion $c' = 9.8$ kPa, unit weight $\gamma = 17.64$ kN/m^3. Different researchers have considered this example using different optimization methods. A summary of the results is given in Table 1. Since the number of slices used for this example is not clearly stated in the literature, we have set the number of slices equal to 15, 20, and 30 while the number of control variables will be 30, 40, and 60, correspondingly. The minimum factors of safety corresponding to different numbers of slices and the associated critical slip surfaces are shown in Table 1 and Fig. 6, respectively. For the results shown in Table 1, it can be considered that all the minimum factors of safety from different researchers are practically the same, except for the result by Malkawi. The critical slip surfaces obtained from the present study are also similar to those by the other researchers, except for the one by Malkawi et al. [13]. The authors have tried GLE and Sarma methods, and the minimum factors of safety are also around 1.32. Finally, when the critical failure surface of Malkawi is analyzed, a factor of safety of 1.37 instead of 1.238 is obtained by the authors. The results obtained by MPSO are very close to those by PSO; however, the number of evaluations required by the former algorithm is much lower than that required by the latter algorithm. The critical slip surfaces derived from PSO and MPSO, as shown in Fig. 6, are also nearly the same.

Table 1
Minimum factors of safety for example 1 (Spencer method)

Optimization method	Minimum factor of safety	NOF
BFGS [18]	1.338	Unknown
DFP [18]	1.338	Unknown
Powell [18]	1.338	Unknown
Simplex [18]	1.339–1.348	Unknown
Pattern search [10]	1.327–1.33	Unknown
Monte Carlo [10]	1.327–1.333	Unknown
Monte Carlo [13]	1.238	Unknown
PSO, number of slices = 15 (this study)	1.3249	54,022
PSO, number of slices = 20 (this study)	1.3285	92,950
PSO, number of slices = 30 (this study)	1.3261	149,830
MPSO, number of slices = 15 (this study)	1.3273	20,021
MPSO, number of slices = 20 (this study)	1.3264	22,146
MPSO, number of slices = 30 (this study)	1.3259	27,856

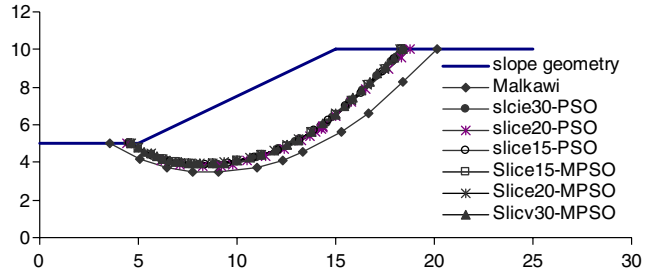

Fig. 6. Summary of critical slip surfaces for the homogenous slope of example 1.

The second example is taken from the work of Bolton et al. [5]. It is the case where a weak layer is sandwiched between two strong layers. The geotechnical properties for soil layers 1–3, respectively, are: friction angle equal to 20°, 10° and 20°; cohesion equal to 28.73 kPa, 0.0 kPa, and 28.73 kPa; unit weight is 18.84 kN/m^3 for all three soil layers. Bolton et al. [5] used Spencer method and Janbu simplified method to calculate the factor of safety and the leap-frog algorithm to locate the critical slip surface. The minimum factors of safety, as well as the location of critical failure surfaces, by Bolton and the authors are very close and are shown in Table 2 and Fig. 7.

The third example is a slope in layered soil, and the genetic algorithm with Spencer method was used by Zolfaghari et al. [20]. The geometric layout of the slope is shown in Fig. 8 while Table 3 gives the geotechnical properties for soil layers 1–4.

The minimum factors of safety were found to be virtually insensitive to the number of slices, which is clearly illustrated in Table 4. Although the number of slices used by Zolfaghari et al. [20] was not clearly stated, the differences in the factors of safety between the results of the authors and Zolfghari are noticeable, and such differences cannot be accounted for by the different number of slices used for computation. As shown in Fig. 9, greater portions of the failure surfaces obtained by the authors lie within soil 3 as compared with the solution by Zolfghari. The lower factors of safety obtained by the authors are hence more reasonable, and the solution by Zolfaghari et al. [20] may be trapped by a local minimum during the

Table 2
Minimum factors of safety for example 2

Optimization method	Minimum factor of safety	NOF
Leap-frog [5]	1.195 (simplified Janbu method)	Unknown
Leap-frog [5]	1.305 (Spencer method)	Unknown
PSO (number of slices = 15)	1.2370 (Spencer method)	92,230
PSO (number of slices = 20)	1.2487 (Spencer method)	102,120
PSO (number of slices = 30)	1.2271 (Spencer method)	132,820
PSO (number of slices = 15)	1.1707 (simplified Janbu method)	65,987
PSO (number of slices = 20)	1.1736 (simplified Janbu method)	103,844
PSO (number of slices = 30)	1.1684 (simplified Janbu method)	131,592
MPSO (number of slices = 15)	1.2079 (Spencer method)	17,327
MPSO (number of slices = 20)	1.2659 (Spencer method)	12,176
MPSO (number of slices = 30)	1.2486 (Spencer method)	16,349
MPSO (number of slices = 15)	1.1789 (simplified Janbu method)	18,334
MPSO (number of slices = 20)	1.1848 (simplified Janbu method)	17,606
MPSO (number of slices = 30)	1.1914 (simplified Janbu method)	24,974

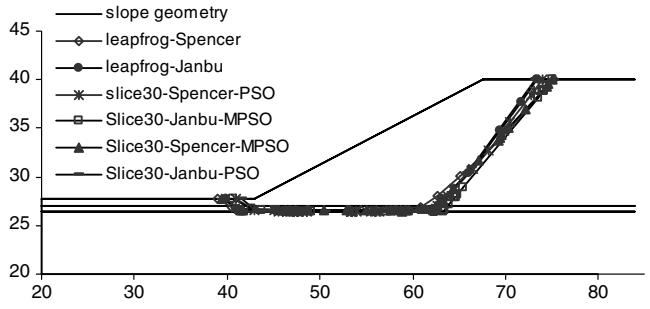

Fig. 7. Critical failure surfaces by Bolton and the authors for a weak layer sandwiched between two strong layers in example 2.

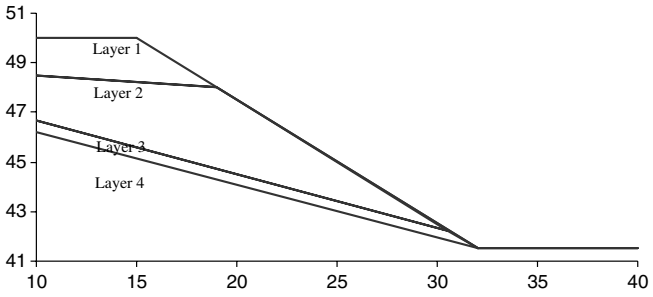

Fig. 8. The slope in layered soil geometry for example 3.

Table 3
Geotechnical parameters for example 3

Layer	γ (kN/m^3)	c (kPa)	ϕ (deg)
1	19.0	15.0	20.0
2	19.0	17.0	21.0
3	19.0	5.00	10.0
4	19.0	35.0	28.0

Table 4
Minimum factors of safety for example 3 (Spencer method)

Optimization method	Minimum factor of safety	NOF
Genetic algorithm [20]	1.24	Unknown
PSO (number of slices = 15)	1.1055	77,995
PSO (number of slices = 20)	1.1095	119,940
PSO (number of slices = 30)	1.1010	131,949
MPSO (number of slices = 15)	1.1139	24,330
MPSO (number of slices = 20)	1.1174	15,925
MPSO (number of slices = 30)	1.1289	14,081

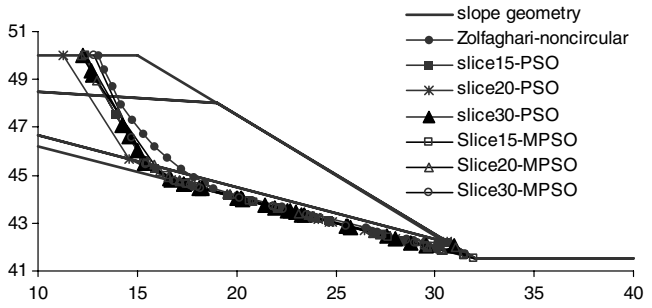

Fig. 9. Summary of critical slip surfaces for example 3.

optimization analysis. Although the results obtained by PSO are slightly smaller than those by MPSO, the number of evaluations required by MPSO was much smaller than that required by the original PSO.

The fourth example is a natural slope with four soil layers as illustrated in Fig. 10, and it has been analyzed by Zolfaghari et al. [20] using the genetic algorithm and Spencer method. The geotechnical parameters for this example are shown in Table 5.

Four loading cases were considered by Zolfaghari et al. [20] in the genetic algorithm minimization: no water

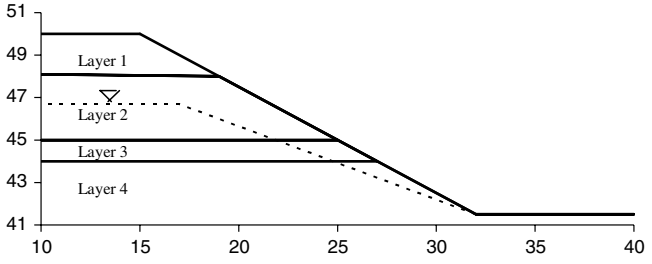

Fig. 10. The geotechnical features of the natural slope with four soil layers in example 4.

Table 5
Geotechnical parameters for example 4

Layer	γ (kN/m^3)	c (kPa)	ϕ (deg)
1	19.0	15.0	20.0
2	19.0	17.0	21.0
3	19.0	5.00	10.0
4	19.0	35.0	28.0

pressure and no earthquake loading (first case); water pressure and no earthquake loading (second case); earthquake loading and no water pressure (third case); water pressure and earthquake loading (fourth case). A pseudo-static horizontal coefficient of earthquake loading of 0.1 has been used in this study. The authors adopted the same number of slices as stated by Zolfghari et al. [20] in the analysis. The results obtained by Zolfghari et al. [20] and the authors are summarized in Table 6 and Figs. 11–14.

The minimum factors of safety for these four cases found by the authors are much lower than those reported by Zolfghari et al. [20]. The critical slip surfaces under each loading case are compared in Figs. 11–14. Under all these cases, more portions of the critical slip surfaces obtained by the authors lie within the weakest layer as compared with the solutions by Zolfaghari et al. [20]. It is possible that the simple genetic algorithm used by Zolfaghari et al. [20] is trapped by the presence of a local minimum so that their results are relatively poor. It is also noticed that static bounds to the control variables are used by Zolfghari et al. [Eq. (1) is not used by Zolfghari to ensure kinematically acceptable failure surfaces are generated], and this can be a possible reason for the relatively poor results from the simple genetic algorithm used by Zolfghari et al. [20]. It is also noticed that the results from the MPSO method are very close to those from PSO, with many fewer computations required. This difficult example has clearly illustrated the effectiveness of the PSO method.

The fifth example is taken from the work of Arai and Tagyo [1], where a layer of low resistance soil is sandwiched between two layers of soil with higher strengths. Geometrical features of the slope and the shear-strength parameters of the various layers are shown in Fig. 15 and Table 7, respectively.

Arai and Tagyo [1] used Janbu simplified method, in combination with the conjugate-gradient method, and obtained a minimum factor of safety of 0.405. The same example was also examined by Sridevi and Deep [17] using a random search technique, and a factor of safety of 0.401

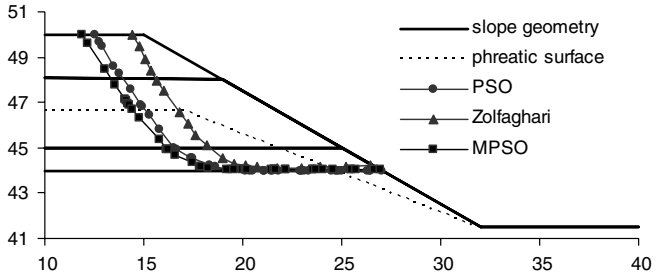

Fig. 11. Critical failure surfaces for example 4 under the first loading case (water pressure and earthquake loading).

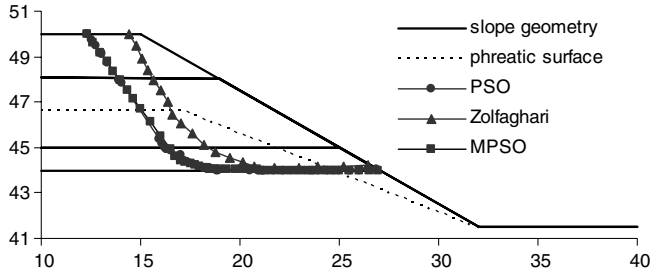

Fig. 12. Critical failure surfaces for example 4 under the second loading case (water pressure and no earthquake loading).

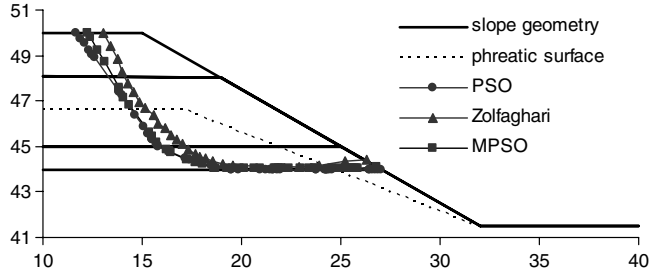

Fig. 13. Critical failure surfaces for example 4 under the third loading case (no water pressure and earthquake loading).

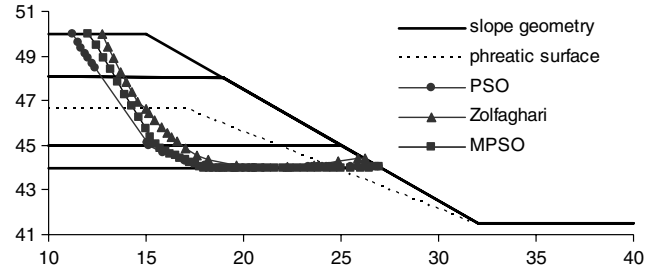

Fig. 14. Critical failure surfaces for example 4 under the fourth loading case (no water pressure and no earthquake loading).

Table 6
Summary of results under each loading case for example 4 (Spencer method)

Loading case	Minimum factor of safety			NOF of this study	
	[20]	PSO	MPSO	PSO	MPSO
Water pressure and earthquake loading (number of slices = 45)	0.98	0.9225	0.9441	160,060	16,835
Water pressure and no earthquake loading (number of slices = 41)	1.36	1.1985	1.2203	114,865	20,722
No water pressure and earthquake loading (number of slices = 44)	1.37	1.0465	1.0592	122,744	14,227
No water pressure and no earthquake loading (number of slices = 40)	1.48	1.3323	1.3490	143,919	14,874

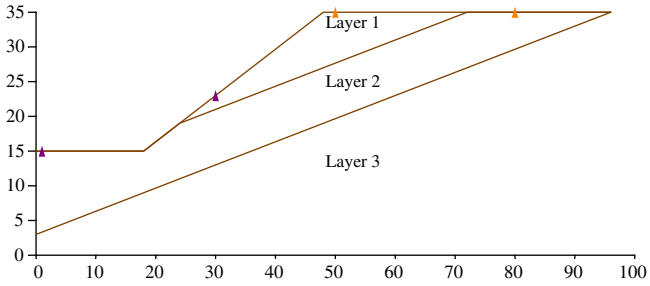

Fig. 15. Cross-section of the layers of example 5, where a layer of low resistance soil is sandwiched between soils of higher strengths.

Table 7
Geotechnical parameters for example 5

Layer	γ (kN/m^3)	c (kPa)	ϕ (deg)
1	18.82	29.4	12.0
2	18.82	9.8	5.0
3	18.82	294.0	40.0

was obtained. Greco [10] used the Monte-Carlo method, and a factor of safety of 0.388 was achieved. Malkawi et al. [13] also adopted the Monte-Carlo technique, and a factor of safety 0.401 was determined and the critical slip surface obtained by Malkawi et al. [13] was very close to that obtained by Greco [10]. It is not clear why a factor of safety 0.388 was reported by Greco, even though the failure surfaces of Greco [10] and Malkawi et al. [13] are virtually the same. Greco's value was also low compared with the results of other researchers. The results of analysis using PSO are shown in Table 8 and Fig. 16.

For the left portion of the failure surfaces, the solutions from different studies were practically the same. The upper segment of the slip surface obtained from this study lies between the solutions of Arai and Tagyo [1] and Sridevi and Deep [17] and those of Greco [10] and Malkawi et al. [13]. It can also been seen from Fig. 16 that all the critical slip surfaces, except those by Greco [10] and Malkawi et al. [13], passed through the stronger soil layer 1 at the right end. The critical slip surfaces from this study intersect soil layer 1 to a small extent instead of to a considerable extent, as obtained by Arai and Tagyo [1] and Sridevi and Deep [17]. When the critical failure surface of Greco [10] is analyzed, the authors obtained a factor of safety of 0.397, instead of 0.388 as reported by Greco. The authors suspect that the low factor of safety obtained by Greco [10] may be due to the tolerance of the iteration analysis, the precision of the calculation and the number of slices used for the analysis. From the results, the authors believe that PSO and MPSO have given satisfactory results for example 5.

Table 8
Summary of minimum factors of safety for example 5 (Janbu simplified method)

Method	Results	NOF
Conjugate gradient [1]	0.405	Unknown
RST-2 [17]	0.401	Unknown
Monte Carlo [10]	0.388	Unknown
Monte Carlo [13]	0.401	Unknown
PSO, number of slices = 15	0.3944	29,877
PSO, number of slices = 20	0.3961	54,404
PSO, number of slices = 30	0.3957	106,193
MPSO, number of slices = 15	0.3963	14,832
MPSO, number of slices = 20	0.3997	13,963
MPSO, number of slices = 30	0.3980	16,422

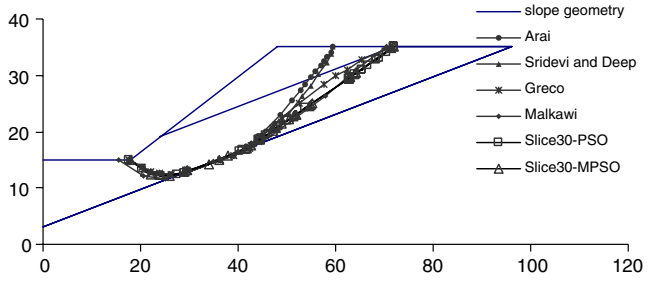

Fig. 16. Comparison of critical slip surfaces for example 5.

Example 6 is a multilayered slope considered by Yamagami and Ueta [18]. The cross section for this example and the geotechnical parameters are shown in Fig. 17 and Table 9, respectively. Yamagami and Ueta [18] examined this example by using Spencer method and different optimization procedures. Greco [10] solved this example using pattern-search and Monte-Carlo techniques. Malkawi et al. [13] also used Spencer method and adopted the Monte-Carlo technique to solve this example. The results of the PSO analysis are shown in Table 10 and Fig. 18.

The results of Yamagami and Ueta [18] using the gradient type method may be slightly less satisfactory, and the methods are possibly trapped by the presence of the local minimum. The results obtained by the authors are in good

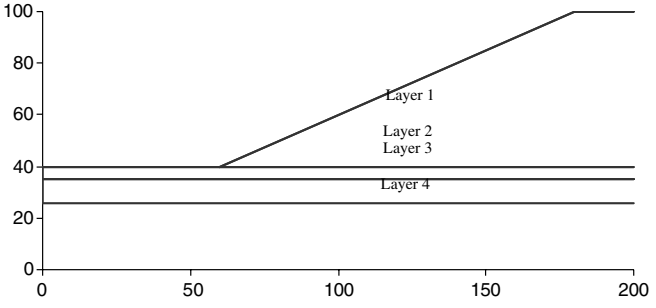

Fig. 17. The geotechnical feature for the multilayered slope of example 6.

Table 9
Geotechnical parameters for example 6

Layer	γ (kN/m^3)	c (kPa)	ϕ (deg)
1	20.38	49.0	29.0
2	17.64	0.0	30.0
3	20.38	7.84	20.0
4	17.64	0.0	30.0

Table 10
Results from different researchers for example 6 (Spencer method)

Method	Minimum factor of safety	NOF
BFGS [18]	1.423	Unknown
DFP [18]	1.453	Unknown
Powell [18]	1.402	Unknown
Simplex [18]	1.405	Unknown
Pattern search [10]	1.400	Unknown
Monte Carlo [10]	1.401	Unknown
Monte Carlo [13]	1.33	Unknown
PSO, number of slices = 15 (this study)	1.3862	41,789
PSO, number of slices = 20 (this study)	1.3942	55,956
PSO, number of slices = 30 (this study)	1.3983	127,260
MPSO, number of slices = 15 (this study)	1.4017	31,024
MPSO, number of slices = 20 (this study)	1.3967	17,787
MPSO, number of slices = 30 (this study)	1.4046	11,773

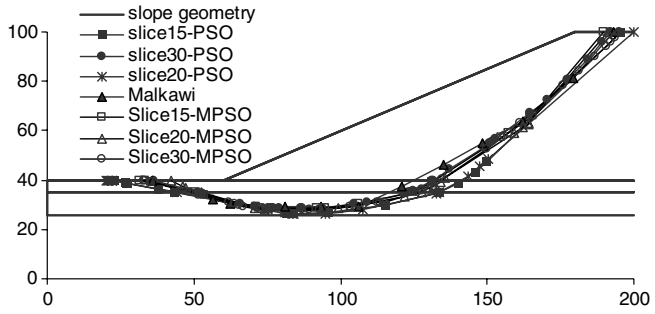

Fig. 18. Comparison of critical slip surfaces for example 6.

agreement with those by Greco [10] and Malkawi et al. [13], and the critical slip surfaces by Malkawi and the authors are shown in Fig. 18. It is observed that the critical slip surface obtained by Malkawi et al. [13] is very close to that from this study when the number of slices equals 30. The factor of safety obtained by the authors is, however, 1.39 for 30 slices, which is different from the value of 1.33 obtained by Malkawi. It can also be concluded that PSO and MPSO have given satisfactory results for example 6.

Example 7, as shown in Fig. 19, is a slope with geotechnical features similar to those in example 3. The thickness

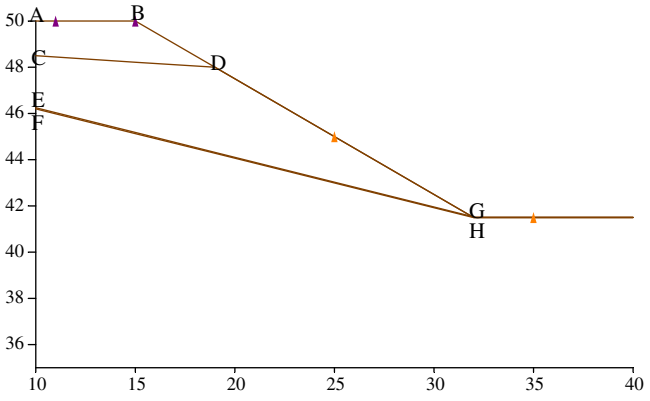

Fig. 19. The cross section of example 7, which has a very thin soft band.

Table 11
Summary of coordinates for key points

Coordinates	*A*	*B*	*C*	*D*	*E*	*F*	*G*	*H*
x-Ordinate	10	15	10	19	10	10	31.9	32
y-Ordinate	50	50	48.5	48.0	46.25	46.2	41.55	41.5

Table 12
Geotechnical parameters for example 7

Layer	γ (kN/m^3)	c (kPa)	ϕ (deg)
1	19.0	15.0	20.0
2	19.0	17.0	21.0
3	19.0	5.00	10.0
4	19.0	35.0	28.0

Table 13
Minimum factors of safety for example 7 (Spencer method)

Different number of slices	Minimum factor of safety	NOF
PSO, number of slices = 15	1.2204	89,744
PSO, number of slices = 20	1.2193	119,563
PSO, number of slices = 30	1.1835	123,326
MPSO, number of slices = 15	1.1876	17,915
MPSO, number of slices = 20	1.2260	15,321
MPSO, number of slices = 30	1.2006	15,153

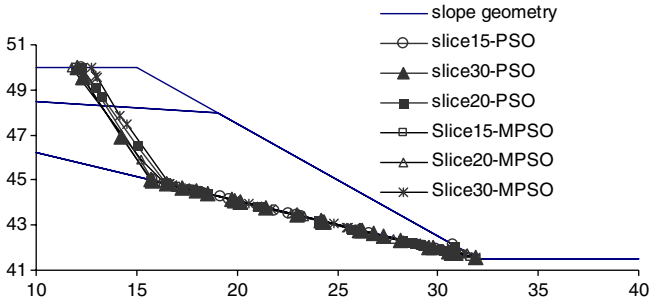

Fig. 20. Comparisons of critical slip surfaces for example 7.

of the thin layer is now reduced to 50 mm so that it is very easy to miss this thin layer under the optimization analysis. The *x*- and *y*-ordinates of the slopes are given in Table 11, while the geotechnical parameters are given in Table 12.

The number of slices is assumed to be 15, 20, and 30 and the results of analyses are shown in Table 13 and Fig. 20. The thickness of this weak layer is only 50 mm, which is much thinner than those used by many other researchers in the literature. The majority of the critical failure surface lies in the weak layer, which is a reasonable result. For this difficult problem with a very thin soft band, both PSO and MPSO have performed well with reasonable results.

6. Convexity of critical failure surface

From the authors' extensive trials and the seven critical failure surfaces examined in this paper, we conclude that

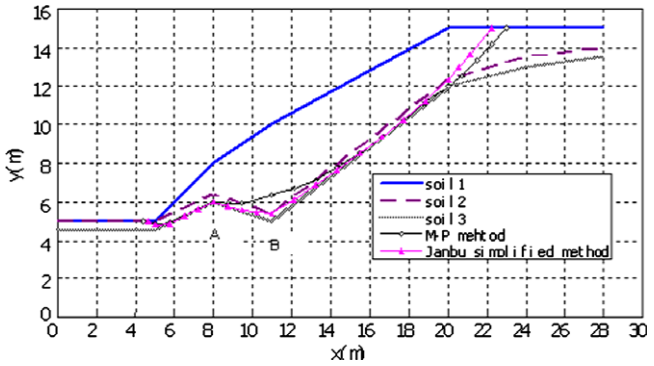

Fig. 21. Critical failure surfaces for a slope with soft band by Janbu simplified method and Morgenstern–Price method.

most critical failure surfaces are convex. The generation of the convex failure surfaces as given in the previous section is adequate enough for most cases. There are, however, some cases where the ground conditions may generate non-convex critical failure surfaces, which have been discussed by Janbu [11], and this is further investigated in this section. Refer to the slope with a middle soft band as shown in Fig. 21. The soil properties for the three soils are: $c' = 4$ kPa, $\phi' = 33°$; $c' = 0$ kPa, $\phi' = 25°$; and $c' = 10$ kPa, $\phi' = 36°$, measured from top to bottom. This slope is analyzed using Janbu simplified method and Morgenstern–Price method, and the critical failure surfaces from the analyses are shown in Fig. 21. The two critical failure surfaces are controlled by the soft band and are similar in location except for section AB. Using Janbu simplified method, which satisfies only force equilibrium, the critical failure surface (FOS = 0.985 without correction factor) basically follows the profile of the soft band even though the kink AB should hinder the failure of the slope. On the other hand, if Morgenstern–Price method is used, the kink AB becomes important in the moment equilibrium and no kink is found for the critical failure surface unless the friction angle of soil 2 is lowered to 20° (a mild kink). This example has illustrated some basic differences in the location of the critical failure surface for simplified and rigorous stability formulations. This result also illustrates that different stability formulations may require different generations of the slip surface algorithm. These kinds of non-convex critical failure surfaces are not commonly encountered but should be allowed in the generation of trial failure surfaces if necessary. The proposed algorithm for the generation of slip surfaces as presented in this paper can achieve this requirement easily by simply eliminating the requirement on the lower bound of each control variable.

7. Conclusions

Minimization of the factor of safety is a classical problem that is still attracting the attention of many engineers and researchers. While classical simplex or gradient methods can work for relatively simple problems, they can easily be trapped by a local minimum. Many researchers are now turning to the modern global optimization methods, which are not limited by the presence of a local minimum during the optimization process.

One of the main limitations of the modern optimization algorithm is the lack of a clear termination criterion. Engineers have to specify a pre-determined number of trials, and the minimum from different trials is taken as the global minimum. Since there is no guideline available for the selection of this pre-determined number of trials, engineers need to specify a large maximum number of trials or use different maximum numbers of trials during the minimization analysis. In this paper, the authors propose a modified PSO method together with a simple termination criterion. Through this modification, a pre-determined number of trials is not required, and the refinement of the search depends on the tolerance of the search as specified by the engineer.

Although the modification to the original PSO method as presented in this paper is not major, the advantages of the present algorithm are clearly illustrated by the numerical examples in this paper. Most of the examples in this study are difficult problems in the global optimization, as the factors of safety are very sensitive to the precise locations of the critical failure surfaces. In addition, when Morgenstern–Price method is used for the analysis, 'failure to converge' is also relatively common and a large value is assigned to those cases that fail to converge (equivalent to a discontinuous objective function), and this will create further difficulties in the search direction. Through the examples in this paper, we have demonstrated that the original and the modified PSO methods are stable in such situations and the results from these methods are also satisfactory.

To demonstrate that the global minimum has been obtained from PSO or MPSO is not easy. The safety map concept of Baker and Leshchinsky [4] can help to verify that the global minimum has been obtained, but this approach requires extensive manual labour and has not been used in this study. The pattern search used by Cheng [9] has been adopted in the verification of the numerical examples in the present study. This approach is not labour intensive but requires very long computer time to try all the possible combinations as specified by the engineers. To reduce the computer time, the authors considered only 15 slices in the optimization analysis. Based on the critical failure surface from PSO/MPSO, each point on the critical failure surface was given 20 possible locations (5×4 grid with a spacing of 0.05 m in the horizontal and vertical directions) and all the combinations were tried. The global minimum obtained from this pattern search is virtually the same as the result from PSO/MPSO for every example in this paper. It can be concluded that PSO and MPSO have performed satisfactorily for all the relatively difficult examples in the present study.

The PSO method is a relatively new global optimization method, which has attracted the attention of several

engineering disciplines, with the exception of civil engineering. The authors have found this method simple to implement. More importantly, an arbitrary initial trial failure surface far from the critical solution can be used for the analysis. This is an important requirement for an automatic scheme in locating the critical failure surface, as a good initial trial for a complicated problem is difficult to define. The authors find that the present proposal works well and is efficient for relatively simple problems. For the more difficult problems, it has been demonstrated in the present study that this method is stable in operation and can work well with poor initial trials. With the proposed algorithm for generation of kinematically acceptable failure surfaces and the PSO, very good results can be obtained within acceptable solution times for many difficult problems with little experience required in operation.

References

[1] Arai K, Tagyo K. Determination of noncircular slip surfaces giving the minimum factor of safety in slope stability analysis. Soils Found 1985;25(1):43–51.
[2] Baker R, Garber M. Theoretical analysis of the stability of slopes. Geotechnique 1978;28:341–95.
[3] Baker R. Determination of the critical slip surface in slope stability computations. Int J Numer Anal Methods Geomech 1980;4:333–59.
[4] Baker R, Leshchinsky D. Spatial distribution of safety factors. J Geotech Geoenviron Eng 2001;127(2):135–45.
[5] Bolton HPJ, Heymann G, Groenwold A. Global search for critical failure surface in slope stability analysis. Eng Optim 2003;35:51–65.
[6] Celestino TB, Duncan JM. Simplified search for non-circular slip surface. In: Proceeding of 10th international conference on soil mechanics and foundation engineering, Stockholm, Sweden, 1981. p. 391–4.
[7] Chen WF. Limit analysis and soil plasticity. USA: Elsevier; 1975.
[8] Chen Z, Shao C. Evaluation of minimum factor of safety in slope stability analysis. Can Geotech J 1983;25(4):735–48.
[9] Cheng YM. Locations of critical failure surface and some further studies on slope stability analysis. Comput Geotech 2003;30:255–67.
[10] Greco VR. Efficient Monte Carlo technique for locating critical slip surface. J Geotech Eng, ASCE 1996;122:517–25.
[11] Janbu N. Slope stability computation. Embankment dam engineering – Cassagrande volume. John Wiley; 1973.
[12] Kennedy J, Eberhart R. Particle swarm optimization. In: Proceeding of the IEEE international conference on neural networks, Perth, Australia, 1995. p. 1942–8.
[13] Malkawi AIH, Hassan WF, Sarma SK. Global search method for locating general slip surface using Monte Carlo techniques. J Geotech Geoenviron Eng 2001;127:688–98.
[14] Nguyen VU. Determination of critical slope failure surfaces. J Geotech Eng, ASCE 1985;111:238–50.
[15] Ourique CO, Biscaia EC, Pinto JC. The use of particle swarm optimization for dynamic analysis in chemical processes. Comput Chem Eng 2002;26:1783–93.
[16] Salman A, Ahmad I, Madani SA. Particle swarm optimization for task assignment problem. Microprocess Microsyst 2002;26:363–71.
[17] Sridevi B, Deep K. Application of global optimization technique to slope stability analysis. In: Proceeding of 6th international symposium on landslides, 1991. p. 573–8.
[18] Yamagami T, Ueta Y. Search for noncircular slip surfaces by the Morgenstern–Price method. In: Proceeding of 6th international conference on numerical methods in geomechanics, 1988. p. 1219–23.
[19] Yin PY. A discrete particle swarm algorithm for optimal polygonal approximation of digital curves. J Visual Commun Image Represent 2004;15:241–60.
[20] Zolfaghari AR, Heath AC, McCombie PF. Simple genetic algorithm search for critical non-circular failure surface in slope stability analysis. Comput Geotechnics 2005;32:139–52.